A SUBJECTIVE SURFACES BASED SEGMENTATION FOR THE RECONSTRUCTION OF BIOLOGICAL CELL SHAPE

Matteo Campana, Cecilia Zanella, Barbara Rizzi

Electronics, Computer Science and Systems Department (DEIS), Bologna University, Bologna, Italy

Paul Bourgine

CREA-Ecole Polytechnique, Paris, France

Nadine Peyriéras

CNRS-DEPSN, Gif sur Yvette, France

Alessandro Sarti

Electronics, Computer Science and Systems Department (DEIS), Bologna University, Bologna, Italy

Keywords: Image Segmentation, Surface Geometry and Shape Extraction, Biological Image Analysis.

Abstract: Confocal laser scanning microscopy provides nondestructive in vivo imaging to capture specific structures that have been fluorescently labeled, such as cell nuclei and membranes, throughout early Zebrafish embryogenesis. With this strategy we aim at reconstruct in time and space the biological structures of the embryo during the organogenesis. In this paper we propose a method to extract bounding surfaces at the cellular-organization level from microscopy images. The shape reconstruction of membranes and nuclei is obtained first with an automatic identification of the cell center and then a subjective surfaces based segmentation is used to extract the bounding surfaces.

1 INTRODUCTION

In vivo imaging of embryo opens the way to a better understanding of complex biological processes at the cellular level. The challenge is to reconstruct at hight resolution the structure and the dynamics of cells throughout the organogenesis and understanding the processes that regulate their behavior. With this studies we expect to be able to measure relevant parameters, such as proliferation rate, highly relevant for investigating anti-cancer drug effects in vivo.

Achieving this goal requires the development of an automated method for extracting the surfaces that represent the cell shapes. We expect to avoid any manual intervention, such as manual cell identifications, which would be a so hight time-consuming process taking into account the huge amount of objects contained in every image.

Sarti et al. (Sarti et al., 2000a), realized a similar study in a previous work where confocal microscopy images were processed to extract the shape of nuclei.

However, in that case, the analysed volumes were not acquired from a living organism but from pieces of fixed tissues. The next sections will introduce the Subjective Surfaces based segmentation algorithm designed to be applied to the living organism scenario.

In Section 2 we illustrate the strategies adopted for image acquisition, filtering and automated cells identification. In Section 3 we describe the segmentation algorithm designed for nucleus and membrane shape reconstruction. The Section 4 briefly explains the technologies utilized for implementing and testing the algorithm. In the last section we show some results.

2 IMAGE ACQUISITION AND PREPROCESSING

High resolution time-lapse microscopy imaging of living organisms is best achieved by multiphoton laser microscopy (MLSM) (Gratton et al., 2001). It allows

imaging the Zebrafish embryo (Megason and Fraser, 2003), engineered with two distinct fluorescent proteins to highlight all nuclei and membranes during early embryonic stages.

Optical sections of the organism are obtained by detecting the fluorescent radiation coming from the laser excited focal plane. The 3-D spatial sampling of the embryo is achieved by changing the focal plane depth. Every image produced is defined on a grid composed by 512 pixels in X and Y direction. The spatial resolution is 0.584793 μm in X, Y and 1.04892 μm in Z. The acquisition of 3-D images has been repeated throughout the early embryonic development, from 3.5 hours post fertilization for 4 hours(at 28^oC) (Kimmel et al., 1995).

The automated or semi-automated reconstruction of the cell contours can be achieved through a procedure consisting of three sequential tasks: filtering, cells detection, and segmentation. The first denoising task should obviously increase the signal-to-noise ratio without corrupt the boundary of cells that should be reconstructed. The geodesic curvature filtering (Sarti et al., 2000a), (Rizzi et al., 2007) has been used to achieve by this task.

A common feature that can be used to identify the cells from images, is the spherical or better the ellipsoidal shape of the nuclei. The goal to recognize the shape of cells has been achieved implementing an algorithm (Melani et al., 2007) based on the generalized 3-D Houg Transform (Ballard, 1981) and able to detecting the centers of the nuclei. The centers have been used separately as the initial condition for the segmentation of every nucleus and membrane.

3 IMAGE SEGMENTATION

We implemented a Subjective Surfaces technique that extracts separately the membranes and nuclei boundaries. This method (Sarti et al., 2000b), (Sarti et al., 2002) is particularly useful for the segmentation of incomplete contours, because it allows the reconstruction and the integration of lacking information. The analysed images, especially the membranes images, are characterized by a signal which is almost undetectable or even absent in some regions. In such situations, the Subjective Surfaces technique should allow the completion of lacking-portions of objects.

3.1 Subjective Surfaces Technique

In order to explain the algorithm, let us consider the 3-D image to be processed $I : (x, y, z) \rightarrow I(x, y, z)$ as a real positive function defined in some domain

$M \subset R^3$. As a first step an initial hypersurface S_i ($S_i : (x, y, z) \rightarrow (x, y, z, \Phi_0)$) is defined in the same domain M of the image I starting from an initial function Φ_0. The algorithm is applied to every single object contained in the images. For every cell, a different function Φ_0 is defined starting from the center of the object detected by the Hough Transform based algorithm. There are some alternative forms for Φ_0, for example $\Phi_0 = -\alpha \mathcal{D}$ or $\Phi_0 = \alpha/\mathcal{D}$, where $\mathcal{D}$ is the 3-D distance function from the reference point.

The Subjective Surfaces technique allows to detect the object shape by evolving the initial function Φ_0 through a flow that depend from the characteristics of the surface S_i and from the local characteristics of the image. As defined in the well-know Geodesic Active Contours technique (GAC) (Caselles et al., 1997) the motion equation which drives the hypersurface evolution is:

$$\Phi_t = gH|\nabla\Phi| + \nabla g \cdot \nabla\Phi; \qquad H = \nabla \cdot \left(\frac{\nabla\Phi}{|\nabla\Phi|} \right) \quad (1)$$

As in GAC the H is the mean curvature except for a parameter ϵ introduced in H expression to weigh the matching of level curves; The edge indicator g is a representation of the structures contained in the image and its gradient is a force field that points in the edges direction.

The entire hypersurface is driven under a speed law dependent on the image gradient, whereas in classical formulation of Level Set methods, as in GAC, the evolution affects only a particular front or level.

The first term on the right side of (1) is a parabolic motion that evolves the hypersurface in normal direction with a velocity weighted by the mean curvature and by the edge indicator g, slowing down near the edges (where $g \rightarrow 0$). The second term on the right is a pure passive advection along the velocity field $-\nabla g$ whose direction and strength depend on position. This term attracts the hypersurface in the direction of the image edges. In regions with subjective contours, continuation of existing edge fragments, ϵ is negligible and (1) can be approximated by a geodesic flow, allowing the boundary completion with curves of minimal length (i.e. straight lines).

A classical expression (Perona and Malik, 1990) of the edge indicator g can be :

$$g(x, y, z) = \frac{1}{1 + (|\nabla G_\sigma(x, y, z) * I(x, y, z)|/\beta)^n} \quad (2)$$

where $G_\sigma(x, y, z)$ is a Gaussian kernel with standard deviation σ, $(*)$ denotes the convolution and n is 1 or 2. The value of g is close to 1 in flat areas ($|\nabla I| \rightarrow 0$) and close to 0 where the image gradient is high (edges). Thus, the minima of g denote the position of edges and its gradient is a force field that can be used

to drive the evolution, because it always points in the local edge direction.

The nuclei and membranes images behave in a completely different way in terms of edge detection: the thickness of membranes signal is about 3 or 4 voxels, whereas nuclei are solid objects. These specific features require using different functions for the detection of edges position in nuclei and membranes images. In nuclei images, the contours to be segmented are located in the regions where image gradient is higher and the minima of (2) denote the position of the edges (Fig. 1(a)). On the contrary, the function (2) can't be applied on membranes images because it reveals a double contour, on the internal and the external side of the cell. An alternative edge indicator has been defined using the image itself (not its gradient) as contours detector. We can use the intensity information to locate the position of the edges, because the membranes images contain high intensity regions, where the labeled membrane structure has been acquired, versus low intensity background regions. The edge indicator we used is:

$$g(x,y,z) = \frac{1}{1 + (|G_\sigma(x,y,z) * I(x,y,z)|/\beta)^2} \qquad (3)$$

As we expected, its minima locate the contours in the middle of the membranes thickness (Fig. 1(b)).

4 IMPLEMENTATION AND VISUAL INSPECTION

The segmentation algorithm has been implemented and tested using a framework designed to visualize and processing 3-D time lapse images (Campana et al., 2007).

The segmented surfaces are extracted as the isosurfaces of the functions Φ obtained after the segmentation. These surfaces are represented and stored through a VTK PolyData format (Schroeder et al., 1998). The segmented surfaces have been superimposed to the original non-processed image (raw data)

(a) Nuclei channel.   (b)   Membranes channel.
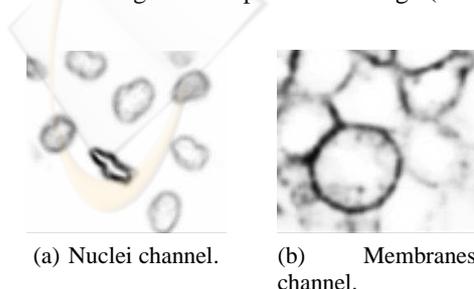
Figure 1: Images of the edge indicators: membranes (a) and nuclei (b).
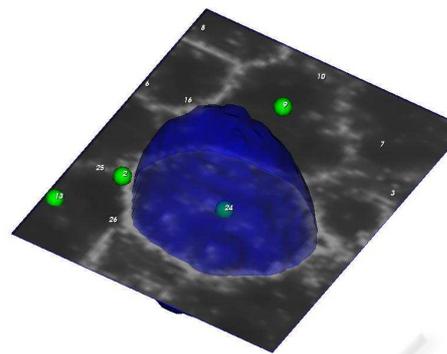
Figure 2: In figure the membrane image is analyzed by a cutting plane, the center of cell number 24 is represented by the green sphere, and its membrane boundary is displayed as a blue surface.

and to detected nuclei in order to easily validate the reconstruction process (Fig. 2). The position of every nucleus detected inside each volume has been represented by a small green sphere labeled by the number that identifies the cell.

The visual inspection realized on preliminary membrane segmented surfaces demonstrated a not exact extraction of the boundaries. This problem occurs in membrane images because they are corrupted by a weak nuclei signal, more intense during mitosis. In order to solve this problem the membranes segmentation requires an additional preprocessing with the goal to remove this interfering signal. First a separation of the nuclei signal from the background is simply obtained by a thresholding of nuclei images. The signal obtained by this thresholding is then used to remove the interfering signal from membranes images.

After segmentation, the intensity distribution of the function Φ is typically associated to a bimodal histogram with a values range between 0 and 255, because of linear rescaling. The highest intensity peak (near to 255) corresponds to the segmented object, the lowest one to the background. The segmented surfaces can be extracted as the isosurfaces corresponding to the intermediate value 128.

5 RESULTS

As we expected the algorithm is able to complete the missing boundaries. the Fig.3 shows the image and the segmented surfaces of dividing membranes during telophase. As is possible observe from the resulting surfaces, the portion of image with missing membrane boundaries, underlined with a red circle, is well completed and extracted.
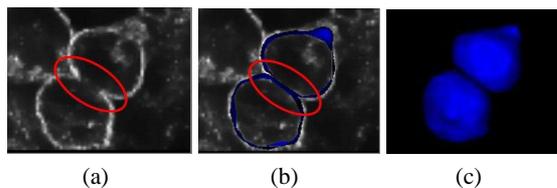
Figure 3: Membrane segmentation of a dividing cell. (a)Membranes signal. (b)Slice of the segmented surfaces. (c)Segmented surfaces.
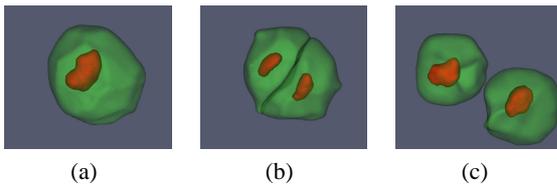
Figure 4: Segmentation of a cell throughout mitosis. Membrane and nucleus shape are respectively represented with green and red surfaces.

(a) Membranes.   (b) Nuclei.

Figure 5: Segmentation of an entire subvolume.

The visual inspection of different segmented surfaces reveals some problems in the reconstruction of objects characterized by flat shapes such as epithelial cells and nuclei of dividing cells. The Fig. 4 show the shape of nuclei and membranes when the cell is close to the division. Before undergoing division, cells become spherical, whereas nuclei staining elongates as the chromosomes arrange in the future cell division plane. It should be noted that the nucleus size is slightly underestimated in the last two parts. This is due to the parabolic regularization term in the motion equation (1), which prevents the segmented surface to reach the contour if it is concave and with high curvature. Excluding these particular shapes the nuclei and membranes surfaces seem to be pretty well reconstructed if compared with the acquired images. In Fig. 5 and Fig. 4 we show some surfaces obtained with the algorithm.

We thank all the members of the Embryomics and BioEmergences projects for our very fruitful interdisciplinary interaction.

REFERENCES

Ballard, D. (1981). Generalizing the hough transform to detect arbitrary shapes. *Pattern Recognition*, 13:111–122.

Campana, M., Rizzi, B., Melani, C., Bourgine, P., Peyriras, N., and Sarti, A. (2007). A framework for 4-d biomedical image processing visualization and analysis. In *GRAPP 08-International Conference on Computer Graphics Theory and Applications*.

Caselles, V., Kimmel, R., and Sapiro, G. (1997). Geodesic active contours. *International Journal of Computer Vision*, 22:61–79.

Gratton, E., Barry, N. P., Beretta, S., and Celli, A. (2001). Multiphoton fluorescence microscopy. *Methods*, 25(1):103–110.

Kimmel, C. B., Ballard, W. W., Kimmel, S. R., Ullmann, B., and Schilling, T. F. (1995). Stages of embryonic development of the zebrafish. *Dev. Dyn.*, 203:253–310.

Megason, S. and Fraser, S. (2003). Digitizing life at the level of the cell: high-performance laser-scanning microscopy and image analysis for in toto imaging of development. *Mech. Dev.*, 120:1407–1420.

Melani, C., Campana, M., Lombardot, B., Rizzi, B., Veronesi, F., Zanella, C., Bourgine, P., Mikula, K., Pe-yrieras, N., and Sarti, A. (2007). Cells tracking in a live zebrafish embryo. In *Proceedings 29th Annual International Conference of the IEEE EMBS*, pages 1631–1634.

Perona, P. and Malik, J. (1990). Scale-space and edge detection using anisotropic diffusion. *IEEE Trans. Pattern Anal. Mach. Intell.*, 12:629–639.

Rizzi, B., Campana, M., Zanella, C., Melani, C., Cunderlik, R., Kriv, Z., Bourgine, P., Mikula, K., Pe-yrieras, N., and Sarti, A. (2007). 3d zebra fish embryo images filtering by nonlinear partial differential equations. In *Proceedings 29th Annual International Conference of the IEEE EMBS*.

Sarti, A., de Solorzano, C. O., Lockett, S., and Malladi, R. (2000a). A geometric model for 3-d confocal image analysis. *IEEE Transactions on Biomedical Engineering*, 47(12):1600–1609.

Sarti, A., Malladi, R., and Sethian, J. A. (2000b). Subjective surfaces: A method for completing missing boundaries. In *Proceedings of the National Academy of Sciences of the United States of America*, pages 6258–6263.

Sarti, A., Malladi, R., and Sethian, J. A. (2002). Subjective surfaces: A geometric model for boundary completion. *International Journal of Computer Vision*, 46(3):201–221.

Schroeder, W., Martin, K., and Lorensen, B. (1998). *The Visualization Toolkit*. Prentice Hall, Upper Saddle River NJ, 2nd edition.